EXPERIMENTAL and MOLECULAR MEDICINE, Vol. 34, No. 6, 411-418, December 2002

Characterization and epitope mapping of two monoclonal antibodies against human CD99

Min Chan Gil[1], Mi-Hong Lee[2], Jeong-In Seo[2], Yoon-La Choi[1], Min-Kyung Kim[3], Kyeong Cheon Jung[4], Seong Hoe Park[1] and Tae Jin Kim[2,5]

[1]Department of Pathology
Seoul National University College of Medicine
Seoul 110-799, Korea
[2]Department of Pathology and Center for Molecular Medicine
Samsung Biomedical Research Insstitute
Sungkyunkwan University School of Medicine
Suwon 440-746, Korea
[3]Department of Pathology
Ilsan Paik Hospital, Inje University College of Medicine
Koyang 411-706, Korea
[4]Department of Pathology
Hallym University College of Medicine
Chunchon 200-702, Korea
[5]Corresponding author: Tel, 82-31-299-6161;
Fax, 82-31-299-6179; E-mail: tjkim@yurim.skku.ac.kr

Accepted 19 November 2002

Abbreviations: Ab, antibody; GST, glutathione *S*-transferase; mAb, monoclonal antibody; PBL, peripheral blood lymphocytes; RU, resonance unit; SPR, surface plasmon resonance

Abstract

CD99 plays an critical role in the diapedesis of monocytes, T cell differentiation, and the transport of MHC molecules. Engagement of CD99 by agonistic monoclonal antibodies has been reported to trigger multifactorial events including T cell activation as well as cell-cell adhesion during hematopoietic cell differentiation. In this study, to identify the functional domains participating in the cellular events, we mapped the epitopes of CD99, which are recognized by two agonistic CD99 monoclonal antibodies, DN16 and YG32. Using recombinant fusion proteins of GST with whole or parts of CD99, we found that both antibodies interact with CD99 molecules independently of sugar moieties. DN16 mAb detected a linear epitope located in the amino terminal region of CD99 while YG32 mAb bound another linear epitope in the center of the extracellular domain. To confirm that the identified epitopes of CD99 are actually recognized by the two mAbs, we showed the presence of physical interaction between the mAbs and the fusion proteins or synthetic peptides containing the corresponding epitopes using surface plasmon resonance analyses. The dissociation constants of DN16 and YG32 mAbs for the antigen were calculated as 1.27×10^{-7} and 7.08×10^{-9} M, respectively. These studies will help understand the functional domains and the subsequent signaling mechanism of CD99.

Keywords: antigens, CD; antibodies, monoclonal; antibody affinity; epitope mapping; epitopes, T lymphocyte

Introduction

CD99 is a 32 kDa cell surface sialomucin-type glycoprotein encoded by the *MIC2* gene that is located in the pseudoautosomal region of the human X and Y chromosomes (Banting *et al.*, 1985; Goodfellow *et al.*, 1986; Aubrit *et al.*, 1989; Gelin *et al.*, 1989). Even though CD99 is broadly distributed on many cell types and expressed on virtually all hematopoietic cell types except granulocytes, the expression density on T-lineage cells seems to be maturation-linked (Dworzak *et al.*, 1994; Dworzak *et al.*, 1999; Park *et al.*, 1999). CD99 was shown to be highly expressed on cortical thymocytes, whereas medullary thymocytes exhibited a relatively weak expression of CD99. Heterogeneity in the level and epitopes of CD99 expression was also observed on peripheral blood lymphocytes (PBL). With distinct CD99 monoclonal antibodies (mAbs), different T cell subsets could be distinguished (Gelin *et al.*, 1991; Dworzak *et al.*, 1994). Interestingly, a restricted epitope of CD99, CD99R, has been defined to be expressed only on T cells, NK cells, and monocytes, but not on B cells, erythrocytes, or platelets (Gelin *et al.*, 1995). These findings that the expression of CD99 was particularly strong on Ewing's sarcoma cells and peripheral primitive neuroectodermal tumors have made CD99 a specific maker of these neoplasms (Hamilton *et al.*, 1988; Kovar *et al.*, 1990; Ambros *et al.*, 1991).

CD99 was initially described as a putative adhesion molecule (termed E2) involved in spontaneous rosette formation of T cells with erythrocytes (Bernard *et al.*, 1988; Aubrit *et al.*, 1989; Gelin *et al.*, 1989; Gelin *et al.*, 1991). Although the function of CD99 is not fully

understood, it has been investigated by using anti-CD99 antibodies to stimulate cells through CD99. Ligation of CD99 on immature (CD4+ CD8+) thymocytes stimulated homotypic aggregation of the cells (Bernard *et al.*, 1995), up-regulation of major histocompatibility (MHC) antigen and T cell receptor (TCR) expression (Choi *et al.*, 1998; Sohn *et al.*, 2001), and apoptosis (Bernard *et al.*, 1997). CD99-induced apoptosis was also noted in Ewing's sarcoma cell lines (Sohn *et al.*, 1998). In Jurkat cells, CD99 engagement resulted in up-regulation of surface LFA-1 (Hahn *et al.*, 1997), while ligation of CD99 on activated and memory T cells stimulates and induces their adhesion to VCAM-1-expressing cell monolayers (Bernard *et al.*, 2000). Although the ligand for CD99 is not yet identified, CD99 is now regarded as one of costimulatory molecules for TCR since CD99 engagement enhanced the signaling of suboptimal CD3 stimulation (Waclavicek *et al.*, 1998). Recently, the role of CD99 in diapedesis of monocytes and motility of cancer cells was suggested (Lee *et al.*, 2002; Schenkel *et al.*, 2002).

We previously developed two anti-CD99 murine monoclonal antibodies, DN16 and YG32, which had been made by immunization of human thymocytes and characterized by expression library screening and transfection studies (Hahn *et al.*, 1997). Interestingly, both antibodies were agonistic in that engagement with DN16 or YG32 mAbs in Jurkat T cells led to activation of mitogen-activated protein kinases (MAPKs) along with homotypic aggregation (Hahn *et al.*, 2000). Here we investigated which epitopes of CD99 interact with the antibodies to exert the effects, since triggering of functional regions of CD99 which include epitopes in the extracellular domain may be responsible for intracellular signaling events. Using various types of glutathione *S*-transferase (GST)-CD99 fusion proteins, we identified the two separately located epitopes recognized by DN16 and YG32 mAbs, respectively. Furthermore, we confirmed the binding of those epitopes with the respective antibodies by surface plasmon resonance (SPR) analysis, and calculated the affinity constants of both antibodies using recombinant antigens. The determination of functional epitopes of CD99 detected by two monoclonal antibodies well be very useful in the elucidation of molecular mechanism of CD99-mediated cell biological events.

Materials and Methods

Materials

The mAbs against CD99, DN16 and YG32, were purchased from DiNonA (Seoul, Korea). Anti-GST antibody was purchased from Pharmacia Biotech (Piscataway, NJ). Anti-mouse IgG horseradish peroxidase conjugates were also purchased from DiNonA. Oligonucleotide primers for PCR were synthesized at Cosmo (Seoul, Korea). Synthetic peptides were synthesized in Peptron (Daejon, Korea).

Construction and expression of CD99 recombinant plasmids

Twenty CD99 recombinant plasmids were constructed by cloning PCR fragments into pGEX-4T-2 vector and pGEX2T (Pharmacia Biotech). All PCR fragments were amplified from a recombinant plasmid containing cDNA of CD99. Primers used for PCR amplification were selected based on the sequence in Genebank and modified to contain *Bam*HI and either *Eco*RI, or *Not*I restriction sites to facilitate cloning (not shown). Both purified PCR products and pGEX-4T-2 vector were digested with *Bam*HI and either *Not*I or *Eco*RI at 37°C overnight, ligated using T4 DNA ligase (Pharmacia Biotech) at 16°C overnight, and then used to transform *E. coli* competent TOP10F' [F' [*lac*Iq, Tn10(TetR)], *mcr*A, D(*mrr-hsd*RMS-*mcr*BC), ϕ80*lac*-ZDM15, Δ*lac*X74, *deo*R, *rec*A1, *ara*D139 D(*ara-leu*) 7697, *gal*K, *rps*L(StrR), *end*A1, *nup*G]. The cloned CD99 sequences were confirmed by DNA sequencing (Macrogen, Seoul, Korea).

E. coli TOP10 cells transformed with the recombinant plasmids were grown at 37°C overnight in Luria broth (LB) medium containing 50 mg/ml ampicillin. The overnight culture was diluted 20 times with fresh LB medium containing the same concentration of ampicillin and grown at 37°C for 3 to 4 h until an optical density value of 0.6 was reached. The gene expression was induced by adding IPTG (Sigma Chemical St. Louis, MO) into the culture to a final concentration of 1 mM. After 4 h of incubation at 37°C with constant shaking, the cells were pelleted by centrifugation at 6000 *g* for 15 min at 4°C and then resuspended with 3 ml of lysis buffer (50 mM Tris, pH 8.0, 1 mM EDTA, 100 mM NaCl) for each gram of packed cells. The suspension was incubated on ice for 30 min with a final concentration of 0.2 mM phenylmethylsulfonyl fluoride (Sigma Chemical).

Western blot analysis of GST recombinant proteins

Aliquots of each lysate of GST-CD99 fusion protein were separated by electrophoresis on 12% SDS-polyacrylamide gels followed by blotting onto nitrocellulose membranes (Schleicher & Schuell, Dassel, Germany). The nitrocellulose membranes were incubated overnight with blocking buffer containing 5% skim milk, 0.05% Tween 20 in PBS and then incubated for 1 h with DN16 or YG32 mAb diluted 1:1000 in blocking buffer. The membranes were rinsed three times with wash buffer (PBS with 0.05% Tween 20) and incubated for 1 h with affinity-purified goat antimouse immunoglobulin G conjugated with

horseradish peroxidase diluted 1:3000 in blocking buffer. After three washes, each reactive protein band was detected by enhanced chemiluminescence (Amersham, Arlington Heights, IL).

SPR analysis

A set of binding experiments was performed with the BIAcore 2000 instrument (BIAcore AB, Uppsala, Sweden), an optical SPR biosensor system (McDonnell, 2001). CM5 sensor chips were used for immobilization of ligands such as anti-GST Ab or anti-CD99 Abs. Briefly, the carboxylated dextran matrix was activated by injecting a mixture of 0.05 M *N*-hydroxysuccinimide (NHS) and 0.2 M *N*-ethyl-*N'*-(3-diethyl aminopropyl) carbodiimide (EDC) (1:1) for 7 min. Ligands were then injected, followed by 1 M ethanolamine hydrochloride (ETH), pH 8.5, to block the remaining NHS ester groups. HBS buffer [10 mM HEPES, 150 mM NaCl, 3.4 mM ethylene-diaminetetracetic acid (EDTA) and 0.005% (v/v) surfactant P20, pH 7.4] was used as the running and dilution buffer in all binding experiments and a pulse of 100 mM HCl or 50 mM NaOH was for regenerations. Results were expressed in resonance units (RU); 1 RU corresponds to a surface mass change of 1 pg protein/mm^2. Non-specific binding to the matrix was eliminated by subtracting the signal obtained on a blank surface (activated carboxymethyldextran saturated with ethanolamine).

For determination of the affinity constants, anti-GST antibody was immobilized on to the CM5 sensor chip surface. Immobilization was performed at a constant flow rate of 5 μl/min at 25°C by addition of reagents in the following sequence: (1) HBS, (2) 35 μl of a mixture of 100 mM NHS and 400 mM EDC in distilled water, (3) 20 μl of anti-GST (50 μg/ml in 10 mM Na-acetate buffer, pH 4.5), (4) residual unreacted active esters were blocked by the injection of 35 μl ETH, pH 8.5, followed by the continuous flow with HBS. Anti-GST mAb was immobilized onto the sensor chip surface resulting in an increase of baseline signal of 1570 RU. Using the anti-GST antibody as a 'entrapping' surface of GST-fusion proteins, the binding procedure of the GST-CD99 fusion protein was performed at a flow rate of 5 μl/min using HBS. GST-CD99 was injected over the anti-GST surface. A sensorgram showing the binding of GST-CD99 onto immobilized anti-GST mAb on the surface of CM5 chip set resulting in an increase of baseline signal of 1700 RU. Antibodies (DN16 or YG32, 25 μl, 100 μg/ml HBS) were then injected to the entrapped GST-CD99 (Figure 3A). Four concentrations for each anti-CD99 mAb were used, ranging from 0 to 168 nM. Dissociation rate constants were calculated by 1:1-binding fitting of the primary sensorgram data using Biaevaluation 2.2.4 software (BIAcore AB, Uppsala, Sweden) assuming a single average dissociation constant. To avoid the influence of changing buffers, data obtained during the first 10-15 s after each injection were omitted from the calculations, and to minimize rebinding effects the dissociation phase was counted just for 30 sec.

SPR analysis using synthetic peptides

A peptide containing the minimal epitope recognized by DN16 or YG32 was synthesized so that Pep-DN16 (GFDLSDALPDNENKKPTAIP) and Pep-YG32 (DDPRPPNPPKPMPNP) were designed to include DN16 and YG32 epitope, respectively. The abilities of these peptides to immobilized anti-CD99 antibodies on the CM5 chip were assessed by peptide injection.

Results

Epitope mapping of GST-CD99 fusion proteins with DN16 and YG32 antibodies

To investigate the epitopes recognized by the two

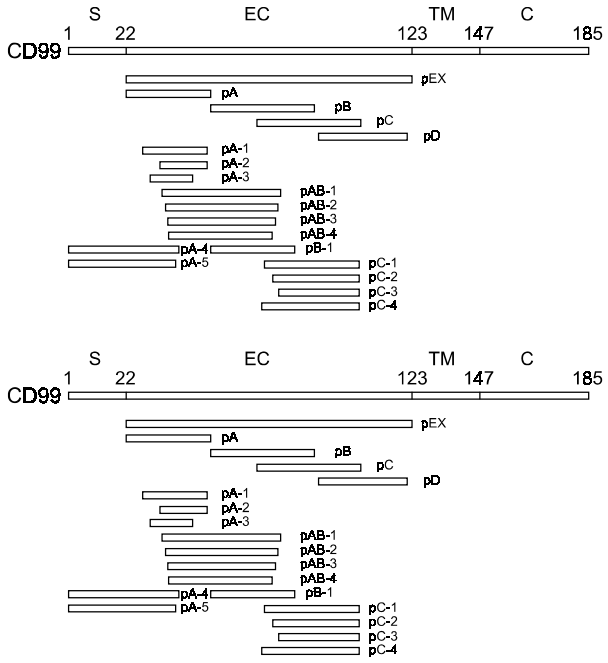

Figure 1. Schematic of the relation of various partial sequence constructs to extracellular domain of CD99. Each construct denotes the various regions of CD99 amplified by PCR from extracellular domain of CD99 and introduced into the pGEX4T-1 vector between *Bam*HI and *Eco*RI site. Locations and lengths of the constructs are tabulated in Table 1. The continuity of the reading frame was confirmed by DNA sequencing. S, signal sequence; EC, extracellular domain; TM, transmembrane domain; C, cytosolic domain.

Table 1. Recombinant GST-CD99 fusion proteins and their immunoblot reactivity to DN16 and YG32.

GST-CD99 fusion protein	Location (a.a.)	Length (a.a)	Immunoblot reactivity	
			DN16	YG32
GST-CD99	1-185	185	O	O
pEX	23-120	98	O	O
pA	23-49	27	O	X
pB	50-87	38	X	O
pC	66-103	38	X	O
pD	88-120	32	X	X
pA-1	26-49	24	O	X
pA-2	32-49	18	O	X
pA-3	29-44	16	O	X
pAB-1	33-75	43	X	O
pAB-2	34-74	45	X	O
pAB-3	35-72	47	X	X
pAB-4	35-73	46	X	X
pB-1	50-80	31	X	O
pC-1	69-103	35	X	X
pC-2	72-103	32	X	X
pC-3	74-103	30	X	X
pC-4	68-103	36	X	O
pA-4	1-39	39	O	X
pA-5	1-38	38	X	X

anti-CD99 monoclonal antibodies, we generated GST fusion proteins encoding different regions of the extracellular domain of CD99 (Figure 1). Twenty different PCR products of CD99 cDNA were run on 2.5% agarose gel, stained with ethidium bromide to confirm their respective sizes, and then cloned into the GST vector at the 3' end (Table 1). Each GST-CD99 fusion clone was transfected into cells, and the lysates expressing these fusion proteins were subjected to Western blot analyses using DN16 or YG32 mAbs. The results of immunoblotting with the 18 different GST constructs are summarized in Table 1. mAb DN16 yielded signals with GST fusion proteins containing the fragments of CD99 amino acid residues 29-49, 32-49, and 1-39, whereas mAb YG32 detected fusion proteins the fragments of the residues 33-75, 34-74, and 68-103 (Figure 2). Since the possible *O*-glycosylation site is located in the residue 63 from the amino terminus of CD99, these results indicate that two epitopes reside in two different regions of the extracellular domain of CD99, which are not related to its sugar moiety. The epitope detected by DN16 mAb (DN16 epitope) was located in the amino terminal region of the CD99 protein, whereas the epitope recognized by YG32 mAb (YG32 epitope) was located in the center of the extracellular part (Figure 1 and Table 1).

To further delineate DN16 and YG32 epitopes, we constructed variants of GST fusion proteins of CD99 among the positive clones by deleting one amino acid residue from each end (Figure 2). The DN16 antibody recognized the fusion proteins corresponding to CD99 amino acid residues 29-49 (pA-2) and 32-49 (pA-3), but not those of 33-75 (pAB-1) and 34-74 (pAB-2). These results indicate that the N-terminal border of the DN16 epitope is leucine at position 32. Moreover, DN16 recognized fusion proteins of 1-39 (pA-4), but not 1-38 (pA-5), indicating that C-terminal border of the DN16 epitope, is lysine residue at position 39 (Figure 2A). On the other hand, YG32 antibody recognized the fusion proteins of 33-75 (pAB-1) and 34-74 (pAB-2), but not of 35-73 (pAB-3) and 35-72 (pAB-4). These results suggest that the N-terminal and C-terminal borders of YG32 epitope are arginine at position 68 and lysine at position 74, respectively. Therefore, the minimal DN16 epitope consists of 8 amino acids LPDNENKK, while the minimal YG32 epitope is RPPNPPK (Figure 2B).

Binding of anti-CD99 antibodies to the GST-CD99 fusion proteins measured by real-time biospecific interaction analysis (BIA)

We performed the real-time BIA analysis, based on SPR technology, to obtain kinetic characteristics of the epitopes. First, we immobilized the GST-CD99 fusion protein through anti-GST antibody that was covalently attached to the CM5 sensor chip surface for efficient exposal of the CD99 antigen to the analyte solution, and assessed its binding ability to each antibody. The amount of immobilized anti-GST antibody was about 1570 RU, and the binding of GST-CD99 fusion protein increased the baseline by 1700 RU. Both monoclonal antibodies bound to the ligand (immobilized GST- CD99) fairly tight, while a control monoclonal antibody did not bind at all (Figure 3). We confirmed whether the same amounts of GST-CD99 were captured after regeneration and reinjection before each experiment for the analyses to be performed in the same conditions. We used four different concentrations of each anti-CD99 antibody to obtain its dissociation constant (K_d). K_d of DN16 and YG32 mAbs for the immobilized GST-CD99 antigen were determined to be 1.27×10^{-7} and 7.08×10^{-9} M at 25°C respectively, indicating that YG32 mAb binds more tightly GST-CD99 than DN16 mAb does at equilibrium.

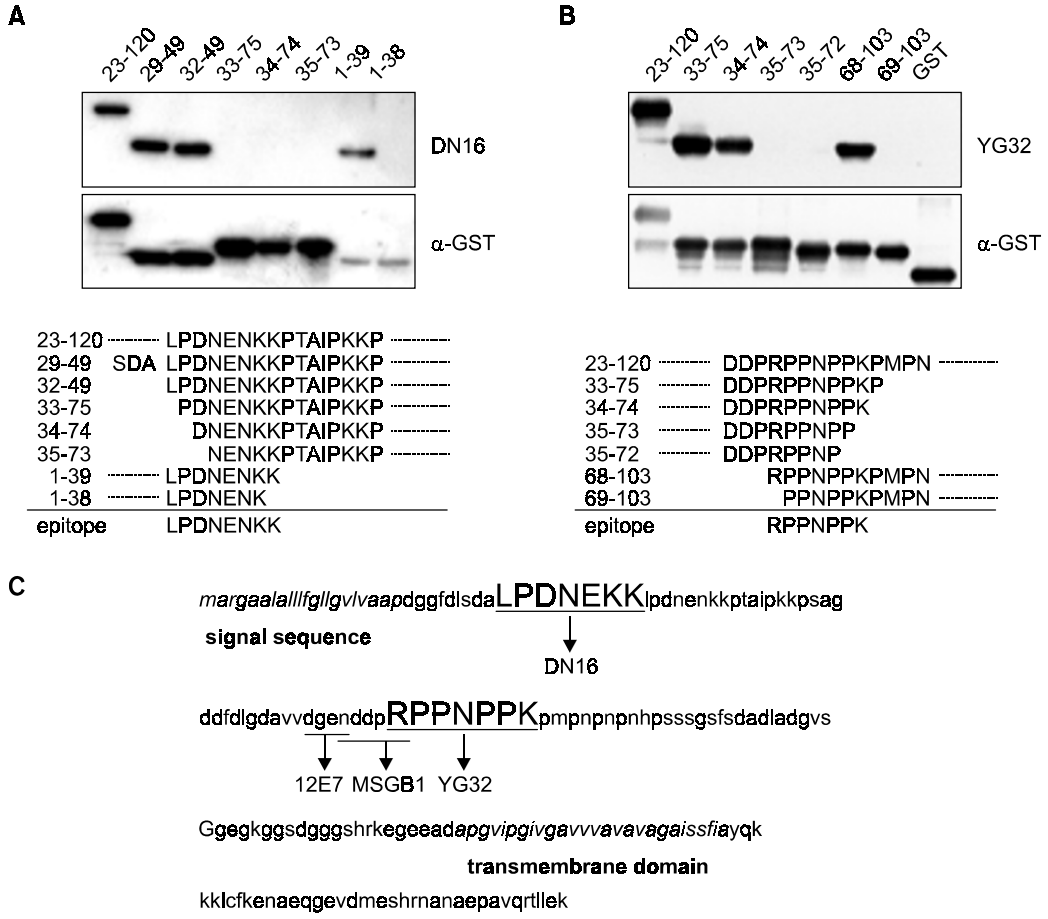

Figure 2. Fine epitope mapping of DN16 and YG32 with western blotting. (A) Western blotting for DN16 epitope mapping; (B) Western blotting for YG32 epitope mapping. *E. coli* lysates harboring plasmids were electrophoresed in 12.5% acrylamide gels and blotted by DN16 and YG32 antibodies. Bands denote the fusion protein as judged with molecular weight protein markers and by Western blots with anti-GST antibody. (C) Locations of epitopes of anti-CD99 mAbs DN16, YG32, 12E7, and MSGB1 on the extracellular domain of CD99.

Specific interaction between CD99 mAbs and the synthetic peptides containing their epitopes

To confirm whether the sequences identified as the epitopes recognized CD99 mAbs in the fusion protein study actually interact with their corresponding mAbs, we performed more BIA analyses. For the experiment, we synthesized two peptides, which contain the DN16 (pep-DN16, GFDLSDALPDNENKKPTAIP) and YG32 epitopes (pep-YG32 DDPRPPNPPKPMPNP), respectively. When DN16 mAb was immobilized on the CM5 chip and the peptides were injected as analyte, DN16 mAb bound specifically only pep-DN16, but not pep-YG32. Similarly, YG32 mAb bound specifically pep-YG32, but not pep-DN16 (Figure 4B), indicating that the interaction is not a nonspecific random event.

Discussion

In this study, we have mapped the antigenic epitopes of CD99 recognized by mAbs, DN16 and YG32. GST fusion proteins with different regions of extracellular domain of CD99 were produced, and subsequent Western blotting and SPR analyses were performed to localize the minimal epitopes. DN16 and YG32 mAbs detected the GST-CD99 proteins expressed in *E. coli* very well, which suggested that both antibodies detected CD99 molecules regardless of the presence of sugar moieties. The DN16 and YG32 epitopes were distinct from epitopes previously reported to bind anti-CD99 mAbs. 12E7 mAb recognized amino acid residues DGEN, and MSGB1 mAb recognized the adjacent stretch of only five amino acid residues NDDPR near YG32 epitope (Figure 2C) (Banting *et al.*, 1989). However, the 12E7 epitope appeared to be present only in a distinct subpopulation of T cells,

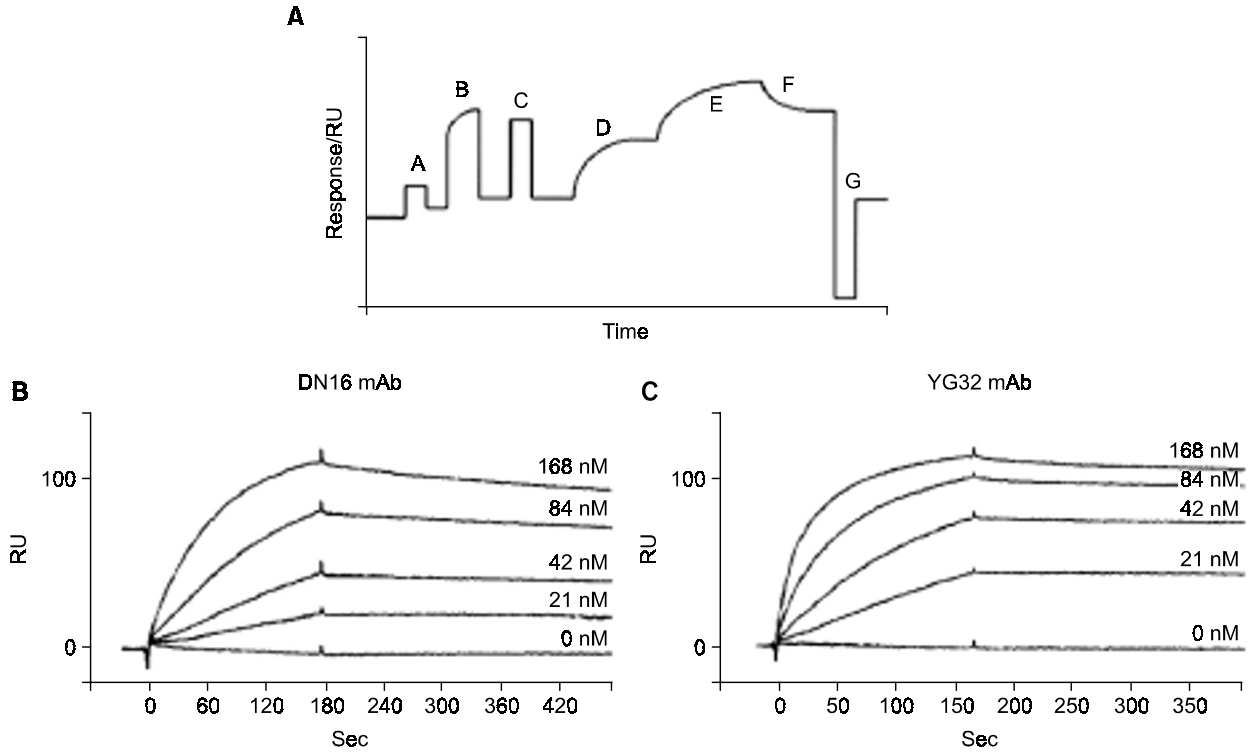

Figure 3. Real time BIA. Sensorgrams showing binding experiments using anti-GST mAb and GST fused CD99 protein (A) Schematic of the strategy. Real time BIA was performed using the following sequential addition of reagents: start, HBS; A, activation of sensor chip surface, 35 μl of a mixture of 100 mM NHS and 400 mM EDC in distilled water; B, binding of anti-GST Ab, 20 μl of anti-GST (50 μg/ml in 10 mM Na-acetate buffer, pH 4.5); C, deactivation of sensor chip surface, 35 μl ETH, pH 8.5 followed by the continuous flow with HBS; D, binding of the GST-CD99 fusion protein at a flow rate of 5 μl/min using HBS; E, binding of antibodies, 25 μl of DN16 or YG32 (100 μg/ml in HBS); F, dissociation of antibodies; G, regeneration of the sensor surface, 5 μl of 10 mM HCl, or 50 mM NaOH. Dose dependence curves for binding of DN16(B) and YG32(C) to the immobilized GST-CD99. DN16 and YG32 were injected at indicated concentrations at a flow rate of 20 ml/min.

while DN16, YG32, O662 and L129 mAbs recognized the whole population of T cells (Gelin *et al.*, 1991). This suggested that the 12E7 epitope may be masked or contributed by sugar moieties present only in the T cell subpopulation, or that the gene segment encoding the 12E7 epitope can be alternatively spliced. Even though we cannot completely exclude the possibility that the sugar moiety contributed partly to the DN16 and YG32 epitopes, it appeared that both antibodies recognized the protein backbone of CD99. This is further supported by the fact that we were able to determine the precise linear epitopes detected by both antibodies. To further define the border of the epitopes, we produced GST-fusion constructs that had N- and C-terminally shortened by one amino acid residue. When the fragments of CD99 were fused with GST, their N-terminal ends were fused directly with the GST protein, whereas C-terminal ends are followed by stop codon. Thus, if the *Bam*HI restriction site at the N-terminal ends of epitopes casually creates glycine or serine, the adjacent amino acid could influence the result of Western blotting. Fortunately, Western blotting showed clear discrimination between constructs, and there was no serine or glycine residue around the N-terminal region of DN16 or YG32 epitope.

The results of epitope mapping by immunoblotting of GST-fusion proteins were substantiated by the SPR analysis. Due to the tight and fast binding of the antibodies to the recombinant antigens, we were able to obtain reliable kinetic (on and off) constants and the dissociation constants. GST-CD99 expressed in bacterial cells binds YG32 mAb more tightly than DN16 mAb (Figure 3B). However, it is not certain whether the affinity differences between the two Abs against GST-CD99 could be applied to the natural form of CD99, which is membrane-bound and glycosylated. Moreover, despite of the recognition of two distantly located epitopes, by what mechanism both of the DN16 and the YG32 epitope ligation independently exert the same functional effects such as upregulation of MHC class I and T cell receptor or homotypic aggregation is not known.

In this report, we elucidated the epitopes reco-

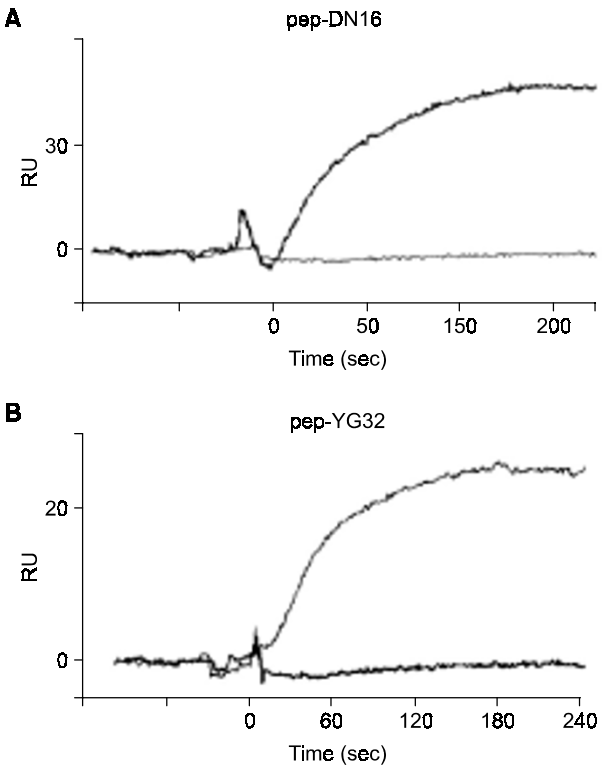

Figure 4. Plots of sensorgrams using peptides. The ability of pep-DN16 and pep YG32 to immobilized anti-CD99 antibodies were assessed. DN16 (A) and YG32 (B) mAbs were directly immobilized to the CM5 chip and the peptides were injected. Black line represented RU value when 1mg of pep-DN16 was injected and gray line represented RU induced by pep-YG32 injection.

gnized by two anti-CD99 antibodies using recombinant fusion proteins of whole or part of CD99 and peptides. The precise localization of antigenic epitopes of agonistic antibodies would be informative regarding the identification of CD99 ligands, since the nature of the ligand is currently elusive. To resolve this issue, the structure of CD99 should be elucidated including the spatial localizations of DN16 and YG32 epitopes in the structure.

Acknowledgments

This work was supported by funds from the 2002 National Research Laboratory Program of Republic of Korea (M1010400012401J00000551).

References

Ambros IM, Ambros PF, Strehl S, Kovar H, Gadner H, and Salzer-Kuntschik M. *MIC2* is a specific marker for Ewing's sarcoma and peripheral primitive neuroectodermal tumors. Evidence for a common histogenesis of Ewing's sarcoma and peripheral primitive neuroectodermal tumors from MIC2 expression and specific chromosome aberration. Cancer 1991;67:1886-93

Aubrit F, Gelin C, Pham D, Raynal B, Bernard A. The biochemical characterization of E2, a T cell surface molecule involved in rosettes. Eur J Immunol 1989;19:1431-6

Banting GS., Pym B, Darling SM, Goodfellow PN. The *MIC2* gene product: epitope mapping and structural prediction analysis define an integral membrane protein. Mol Immunol 1989;26:181-8

Banting GS, Pym B, Goodfellow PN. Biochemical analysis of an antigen produced by both human sex chromosomes. EMBO J 1985;4:1967-72

Bernard A, Aubrit F, Raynal B, Pham D, Boumsell L. A T cell surface molecule different from CD2 is involved in spontaneous rosette formation with erythrocytes. J Immunol 1988;140:1802-7

Bernard G, Breittmayer JP, de Matteis M, Trampont P, Hofman P, Senik A, Bernard A. Apoptosis of immature thymocytes mediated by E2/CD99. J Immunol 1997;158: 2543-50

Bernard G, Raimondi V, Alberti I, Pourtein M, Widjenes J, Ticchioni M, Bernard A. CD99 (E2) up-regulates $\alpha 4\beta 1$-dependent T cell adhesion to inflamed vascular endothelium under flow conditions. Eur J Immunol 2000;30:3061-5

Bernard G, Zoccola D, Deckert M, Breittmayer JP, Aussel C, Bernard A. The E2 molecule (CD99) specifically triggers homotypic aggregation of CD4+CD8+ thymocytes. J Immunol 1995;154:26-32

Choi EY, Park WS, Jung KC, Kim SH, Kim YY, Lee WJ, Park SH. Engagement of CD99 induces up-regulation of TCR and MHC class I and II molecules on the surface of human thymocytes. J Immunol 1998;161:749-54

Dworzak, MN, Fritsch G, Buchinger P, Fleischer C, Printz D, Zellner A, Schollhammer A, Steiner G, Ambros PF, Gadner H. Flow cytometric assessment of human *MIC2* expression in bone marrow, thymus, and peripheral blood. Blood 1994;83:415-25

Dworzak MN, Fritsch G, Fleischer C, Printz D, Frschl G, Buchinger P, Mann G, Gadner H. CD99 (*MIC2*) expression in paediatric B-lineage leukaemia/lymphoma reflects maturation-associated patterns of normal B-lymphopoiesis. Br J Haematol 1999;105:690-5

Gelin C, Aubrit F, Phalipon A, Raynal B, Cole S, Kaczorek M, Bernard A. The E2 antigen, a 32 kd glycoprotein involved in T-cell adhesion processes, is the *MIC2* gene product. EMBO J 1989;8:3253-9

Gelin C, Zilber MT, Jovanovic D, Boumsell L. Leucocyte Typing V, 1995, 283-84, Oxford University Press, New York, NY

Gelin C, Zoccola D, Valentin H, Raynal B, Bernard A. Isoforms of the E2 molecule: D44 monoclonal antibody defines an epitope on E2 and reacts differentially with T cell subsets. Eur J Immunol 1991;21:715-9

Goodfellow PJ, Darling SM, Thomas NS, Goodfellow PN. A

pseudoautosomal gene in man. Science 1986;234:740-3

Hahn JH, Kim MK., Choi EY, Kim SH, Sohn HW, Ham DI, Chung DH, Kim TJ, Lee WJ, Park CK, Ree HJ, Park SH. CD99 (*MIC2*) regulates the LFA-1/ICAM-1-mediated adhesion of lymphocytes, and its gene encodes both positive and negative regulators of cellular adhesion. J Immunol 1997;159: 2250-8

Hahn MJ, Yoon SS, Sohn HW, Song HG, Park SH, Kim TJ. Differential activation of MAP kinase family members triggered by CD99 engagement. FEBS Lett 2000;470:350-4

Hamilton G, Fellinger EJ, Schratter I, Fritsch A. Characterization of a human endocrine tissue and tumor-associated Ewing's sarcoma antigen. Cancer Res 1988;48:6127-31

Kovar H, Dworzak M, Strehl S, Schnell E, Ambros IM, Ambros PF, Gadner H. Overexpression of the pseudoautosomal gene *MIC2* in Ewing's sarcoma and peripheral primitive neuroectodermal tumor. Oncogene 1990;5:1067-70

Lee HJ, Kim E, Jee B, Hahn JH, Han K, Jung KC, Park SH, Lee H. Functional involvement of src and focal adhesion kinase in a CD99 splice variant-induced motility of human breast cancer cells. Exp Mol Med 2002;34:177-83

McDonnell JM. Surface plasmon resonance: towards an understanding of the mechanisms of biological molecular recognition. Curr Opin Chem Biol 2001;5:572-7

Park CK, Shin YK, Kim TJ, Park SH, Ahn GH. High CD99 expression in memory T and B cells in reactive lymph nodes. J Korean Med Sci 1999;14:600-6

Schenkel AR, Mamdouh Z, Chen X, Liebman RM, Muller WA. CD99 plays a major role in the migration of monocytes through endothelial junctions. Nat Immunol 2002;3:143-50

Sohn HW, Choi EY, Kim SH, Lee IS, Chung DH, Sung UA, Hwang DH, Cho SS, Jun B H, Jang JJ, Chi JG, Park SH. Engagement of CD99 induces apoptosis through a calcineurin-independent pathway in Ewing's sarcoma cells. Am J Pathol 1998;153:1937-45

Sohn HW, Shin YK, Lee IS, Bae YM, Suh YH, Kim MK, Kim TJ, Jung KC, Park WS, Park CS, Chung DH, Ahn K, Kim IS, Ko YH, Bang YJ, Kim CW, Park SH. CD99 regulates the transport of MHC class I molecules from the Golgi complex to the cell surface. J Immunol 2001;166:787-94

Waclavicek M, Majdic O, Stulnig T, Berger M, Sunder-Plassmann R, Zlabinger GJ, Baumruker T, Stöckl J, Ebner C, Knapp W, Pickl WF. CD99 engagement on human peripheral blood T cells results in TCR/CD3-dependent cellular activation and allows for Th1-restricted cytokine production. J Immunol 1998;161:4671-8